Soft Matter

Accepted Manuscript

ROYAL SOCIETY OF CHEMISTRY

www.rsc.org/softmatter

Journal Name

RSCPublishing

ARTICLE

The potential of F127-water soft system towards selective solubilisation of Iridium(III) octahedral complexes

Cite this: DOI: 10.1039/x0xx00000x

Received 00th January 2012,
Accepted 00th January 2012

DOI: 10.1039/x0xx00000x

www.rsc.org/

Anna Maria Talarico,[a] Elisabeta Ildyko Szerb,[a,b] Mauro Ghedini,[a,c] and Cesare Oliviero Rossi[a *]

In order to obtain new functional soft systems to be used as templating agents for the construction of functional mesostructured materials, the dynamic orderered soft systems formed by an hydrophilic ionic iridium(III) complex (***IrPa***) embedded into two different concentration F127-water mixtures has been investigated. To this aim, combined spectral and time-resolved photophysical techniques and rheological methods, have been employed. The position of the chromophore inside the micellar, cubic and hexagonal phases of the F127 polymeric neutral surfactant in water was effectively determined. The hydrophilic character of the iridium(III) complex chosen, allowed the preferentially functionalization of the F127 corona in the micellar and cubic phases.

Introduction

Soft complex ordered systems are currently widely used in many remarkable studies in different fields of modern research. In particular, they are increasingly investigated as solubilizing delivery drug systems in medicine and pharmaceutics[1], nanocarriers in food industries[2] or as templates for the construction of functional ordered nanomaterials in biomedical or materials sciences.[3] Commonly, the systems under study are ordered lyotropic phases formed by common surfactants in water that host the functional molecule, the surfactant having the role principally to order, deliver and protect the guest. One of the targeted systems is a class of triblockcopolymeric organic neutral surfactants, formed by different ratios of poly(ethylene oxide) (PEO) and poly(propylene oxide) (PPO) groups namely Poloxamers or Pluronics, due to their remarkable association properties in water, large solubilization capacities, biocompatibility and thermosensitivity.[4,5] Very important, the phase diagram of these neutral surfactants is highly sensitive to the presence of guest molecules.[6] Moreover, when these systems are used as templates, the position of the functional molecules is essential for the final properties of the materials obtained. Therefore, it becomes evident the importance of studying such kind of soft systems also in an attempt to program the properties of the final material by engineering the initial template.

From the large family of Pluronic surfactants, F127 $(PEO)_{100}$-$(PPO)_{70}$-$(PEO)_{100}$ copolymer is typically employed for the synthesis of mesoporous titania materials.[3e,7] F127 form micelles in water comprising of hydrophobic PPO blocks as the core and hydrated PEO blocks as the hydrophilic corona.[4,8] On further increase of concentration and/or temperature, it organize into a highly viscous phase with a solid-like behaviour, reported as a discrete cubic phase.[8,9] Therefore, the guest has different microenvironments to locate as a function of its hydrophobic or hydrophilic character, and as a consequence of its surroundings, may show quite different physical and chemical properties. In this context, iridium(III) complexes are extremely useful, their photophysical properties being strongly affected by changes of molecular surrounding in terms of intermolecular interactions, environmental polarity and medium rigidity.[10] This peculiar behaviour allows their successful employment also in the probing micellar systems.[10c,f-11]

In a previous study, we determined the position of a phosphorescent amphiphilic ionic iridium(III) emitter (***Ir12***) (Figure 1), scarcely soluble in water, in the soft phases of the neutral Pluronic F127 surfactant, by using combined spectral and time-resolved photophysical techniques and rheological methods.[11a]

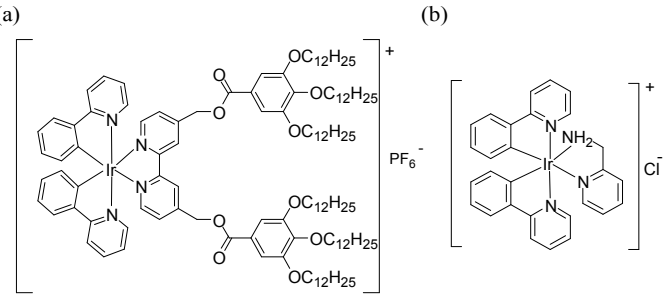

Figure 1. (a) Chemical structure of the amphiphilic ionic iridium(III), ***Ir12***; (b) Chemical structure of the iridium(III) complex, ***IrPa***.

To enhance the solubility of the complex, THF was added as co-solvent. In this system, we observed the preferential location of the iridium(III) emitter inside the micellar core at lower concentrations and its displacement towards the hydrophilic corona of the micelles with the increasing of concentration.

Herein, we investigated the behaviour of an iridium(III) ionic complex (***IrPa***), soluble in water, whose chemical structure is presented in Figure 1, embedded in F127-water system.

For the surfactant-water system, two borderline concentrations were chosen, 15% and 18% w/w respectively, where the transition from micellar phase to cubic phase is around 25-30°C. As shown before, these concentrations will allow huge responses also to small perturbations in terms of structural organization of the system, in a temperature range close to room temperature.[11a] Indeed, these two isoplethal lines permit a judicious examination of the structural changes on passing from molecular to micellar, cubic and hexagonal phases, evidencing better the influence of the molecular guest present in the mixtures. Furthermore, low concentration cubic and hexagonal phases are formed with temperature, permitting thus a more facile structural characterisation of the system components.

The same quantity of chromophore was added to both systems (molality ***IrPa*** = $4.3 \cdot 10^{-4}$mol/kg; mole ratios ***IrPa*** / F127 = 1 / 6.7 for system ***Sol1*** and 1 / 8.3 for system ***Sol2***). The loaded systems and their blank solutions were investigated by differential scanning calorimetry (DSC), rheological measurements, diffusion NMR experiments and photophysical investigation.

Experimental section

Materials and measurements.

All commercially available starting materials were used as received without further purification. Complex ***IrPa*** was synthesized as previously reported.[12] The Pluronic F127 poly(ethylene oxide)$_{100}$-poly(propylene oxide)$_{70}$-poly(ethylene oxide)$_{100}$ (PEO-PPO-PEO) copolymer, with an average molecular weight of 12 600 and 70% poly-(ethylene oxide) composition, was supplied by Sigma-Aldrich and used as received.

Samples preparation. Two stock solutions of F127 in water of 15% w/w (***Sol1***: 50 g H_2O + 8.835 g F127) and 18% w/w (***Sol2*****:** 50 g H_2O + 10.980 g F127) respectively, were prepared previously. The solutions were stirred at 0-5°C for 24 hours, and then 0.0139 g ***IrPa*** were added for 11.767 g ***Sol1*** (system ***IrPa_Sol1)*** and for 12.20 g ***Sol2*** (system ***IrPa_Sol2***) respectively. The latter solutions were stirred 2 more days at 5°C. Molality ***IrPa*** = $4.3 \cdot 10^{-4}$mol/kg for both systems; mole ratios ***IrPa*** / F127 = 1 / 6.7 for system ***Sol1*** and 1 / 8.3 for system ***Sol2***).

NMR diffusion. Spectra were acquired on a Bruker NMR spectrometer AVANCE 300 Wide Bore working at 300 MHz on 1H. The employed probe was a Diff30 Z-diffusion 30 G/cm/A multinuclear with substitutable RF inserts. Spectra were obtained by applying the Fourier transform to the resulting free induction decay (FID) of a single π/2 pulse sequence. The π/2 pulse width was about 8 μs. Pulsed field gradient spin-echo (PFG-SE) method was used to measure the self-diffusion coefficients (D). This technique, first proposed by Stejskal and Tanner,[13] consists of a Hahn-Echo pulse sequence ($\pi/2-\tau-\pi$) with two identical magnetic field gradient pulses, the first applied between the $\pi/2$ and π rf pulse (during the dephasing) and the second after the π rf pulse (during the rephasing) but before the echo. Following the usual notation, the magnetic field pulses have magnitude g, duration δ, and time delay Δ. The attenuation of the echo amplitude is represented by the Stejskal-Tanner equation (1):

$$A(g) = \exp[-\gamma^2 g^2 D \delta^2 (\Delta - (\delta/3)] \quad (1)$$

where D is the self-diffusion coefficient and γ is the nuclear gyromagnetic ratio. Note that the exponent in the equation is proportional to the mean-squared displacement of the molecules over an effective time scale (Δ - (δ/3). For the investigated samples, the experimental parameters Δ and δ, ranged between 20-25 ms and 1-4 ms, respectively. The gradient amplitude, g, varied from 10 to 850 G cm^{-1}. In this condition the uncertainty in the self-diffusion measurements is ~ 3%.

Finally, longitudinal relaxation times (T2) were measured by the Carr-Purcell-Meiboom-Gill (CPMG) sequence that is derived from the Hahn spin-echo sequence. This sequence is equipped with a "built-in" procedure to self-correct pulse accuracy error. NMR measurements were run by increasing temperature step by step from 10 to 80 °C, with steps of 5 °C, and leaving the sample to equilibrate for about 20 min.

^{1}H-NMR relaxation times (T2) were obtained from F127 methyl protons by means of signal decay on Hahn spin echo sequences.[14] A nonlinear least-squares fitting procedure was used to get T2 values. The temperature was controlled to ± 0.5 °C and calibrated with a copper–constantan thermocouple. Sample rotation was set at 20 Hz.

DSC measurements. DSC has been used in this research for the measurement of the order–disorder transition temperature. The experiments were performed on the samples by using a Setaram micro DSC III instrument. The indium was used to

calibrate temperature and energy scales. Samples (20-30 mg) were sealed in aluminum-cells and brought to the initial temperature. As a reference, a sealed pan with the corresponding amount of heavy water was used. To check water evaporation, the pans have been weighed before and after the DSC measurements. The DSC thermograms were recorded in the temperature range from 5 to 80°C. The heating rate was 1°C·min^{-1}. Thermograms were digitized by an IBM computer, which allowed the determination of the phase transition temperatures with the associated heat changes by the use of the commercial software Origin 7.5 (OriginLab, MA USA).

Rheology. Rheological measurements were carried out using a shear strain controlled rheometer RFS III (Rheometrics, USA) equipped with a cuvette, cylinder geometry (external and inner radius of 18 and 17 mm, respectively). The temperature was controlled by a water circulator apparatus (±0.2°C). To prevent errors due to evaporation, measuring geometry was surrounded by a solvent trap containing water. Steady flow experiments were performed in the shear rate range of 1–1000 s^{-1}. To ensure steady flow conditions, the required equilibration time was determined by transient experiments, according to step-rate tests. Ten second perturbations ensured steady flow conditions in the system for the whole shear rate range. The rheological behaviour at different temperatures has been investigated by a time cure test at 1 Hz with a heating ramp rate of 1°C·min^{-1}. The small amplitude dynamic tests provided information on the linear viscoelastic behaviour of materials through the determination of the complex shear modulus:

$$G^*(\omega) = G'(\omega) + iG''(\omega) \quad (2)$$

or in terms of complex viscosity,

$$\eta^* = \frac{G^*(\omega)}{\omega} \quad (3)$$

where G'(ω) is the in phase component, G"(ω) is the out-of-phase component, and *i* is the imaginary unit of the complex number. G'(ω) is a measure of the reversible, elastic energy, while G"(ω) represents the irreversible viscous dissipation of the mechanical energy.[15] The dependence of these quantities on the temperature gives rise to the so-called time cures. The applied strain amplitude for the viscoelastic measurements has been reduced until the linear response regime has been reached. This analysis has been made by performing strain sweep tests in all investigated temperature range.

Photophysics. Spectrofluorimetric grade solvents (Acros Organics) were used for the photophysical investigations in solution. Steady-state emission spectra were recorded on a Horiba Jobin Yvon Fluorolog 3 spectrofluorimeter, equipped with a Hamamatsu R-928 photomultiplier tube.

Emission quantum yields of ***IrPa*** in water was determined using the optically dilute method on solutions whose absorbance at excitation wavelengths was <0.2; $Ru(bpy)_3Cl_2$ (bpy = 2,2'- bipyridine) in H_2O was used as standard (ϕ = 0.028).[16] The experimental uncertainty on the emission quantum yields is 10%.

The emission quantum yields of ***IrPa_Sol1*** and ***IrPa_Sol2*** mixtures, both at 25°C and as a function of temperature, were obtained by means of a 102 mm diameter integrating sphere coated with Spectralon® and mounted in the optical path of the spectrofluorimeter using, as excitation source, a 450 W Xenon lamp coupled with a double-grating monochromator for selecting wavelengths. The experimental uncertainty on the emission quantum yields is 5%.

Time-resolved measurements were performed using the time-correlated single-photon counting (TCSPC) option on the Fluorolog 3. NanoLED at 370 nm, fwhm < 200 ps , was used to excite the sample. Excitation sources were mounted directly on the sample chamber at 90° to a single-grating emission monochromator (2.1 nm mm^{-1} dispersion; 1200 grooves mm^{-1}) and collected with a TBX-04-D single-photon-counting detector. The photons collected at the detector were correlated by a time-to-amplitude converter (TAC) to the excitation pulse. Signals were collected using an IBH Data Station Hub photon counting module and data analysis was performed using the commercially available DAS6 software (HORIBA Jobin Yvon IBH). Goodness of fit was assessed by minimizing the reduced Chi squared function (χ^2) and visual inspection of the weighted residuals.

To reach the mesophase, the samples were heated in the sample compartment of the spectrofluorimeter for steady state and time resolved luminescence measurements and in the sample compartment of the integrating sphere for the luminescence quantum yield determination by means of a customized hot stage realized by CaLCTec s.r.l. (Rende, Italy)

Results and discussion

The micellar structure, lyotropic behaviour and phase diagram of F127 in water was intensively studied over the last 20 years, by means of various physical chemistry and structural techniques.[8,9,11a] It was showed that, at low concentration and temperature, the unimers are fully dissolved Gaussian chains, and upon the critical micellar concentration (*cmc* = around 4·10^{-4} mol·L^{-1}), aggregates via a dehydration mechanism of the PPO blocks, into spherical micelles that consist of hydrophobic PPO cores and hydrated PEO corona shells. The dimensions of the micelles are only temperature dependent. Around r.t., the micelles close pack into a highly viscous cubic phase, *via* a 'hardsphere crystallisation' mechanism. At higher temperatures (over 65°C), the system viscosity decreases drastically because of the PEO partial dehydration, the micelles shape change to prolate ellipsoid, and a hexagonal packing is achieved.

DSC analysis. The heat flow vs. temperature analysis was performed on both ***IrPa _Sol1*** and ***IrPa _Sol2*** mixtures and on their corresponding blank solutions ***Sol1*** and ***Sol2***. The plots showed the occurrence of the characteristic broad endothermic peak of the F127-water system previously reported, ascribed to the well investigated micellar formation process.[5d,9a,c,d] The DSC data is summarized in Table 1.

Table 1. DSC data for the investigated samples.

	$\Delta H \pm 0.1$ [a] (J/g)	$T_{on} \pm 0.1$ [b] (°C)	$T_m \pm 0.1$ [c] (°C)
Sol1	3.8	15.4	18.3
IrPa_Sol1	4.1	14.9	18.0
Sol2	4.4	13.6	16.8
IrPa_Sol2	4.4	13.6	16.9

[a]Micellization enthalpy values; [b]Temperature data as onset peaks; [c]Temperature data as maximum of the peaks.

In the case of system 1, it has been found that the micelle formation temperature decreases slightly with the introduction of the ***IrPa*** chromophore in the system, whereas the area of the endothermic peak slightly increases. For system 2, the higher content of polymer seems to overlap the effect of ***IrPa***, the characteristics of the F127-water prevailing. The thermograms show that the micellar formation process may be considered complete for all systems at 28°C. Consequently, from this temperature value, the increase of the complex viscosity can be interpreted in terms of micellar growth. Additionally, the calorimetric measurements showed that none of the mixtures undergo to other enthalpy change associated to the transition in the gel phase, in agreement with what already reported in literature.[5d,9]

Rheology. In Table 2 is presented the temperature dependence of the Newtonian viscosity for both iridium containing mixtures (***IrPa_Sol1*** and ***IrPa_Sol2***) and for their corresponding blank solutions (***Sol1*** and ***Sol2***). All the mixtures analyzed show a Newtonian behaviour in the liquid region characterized by an independency of viscosity with shear rate.

Table 2. The Newtonian viscosity as a function of temperature.

	Viscosity ± 0.0001 [Pa·s]			
	10°C	15°C	20°C	25°C
Sol1	0.0210	0.0167	0.0227	0.0618
IrPa_Sol1	0.0212	0.0168	0.0243	0.0642
Sol2	0.0272	0.0229	0.0581	Thinning
IrPa_Sol2	0.0288	0.0253	0.0665	Thinning

Two relevant features emerge: low viscosity values and a progressive increase with increasing temperature. These findings clearly suggest the presence of a molecular solution at low temperature and its transformation into a micellar phase with spherical aggregates that progressively grow with temperature. Near the cubic phase, the mixtures show also a Newtonian behaviour, but the viscosity is too high to correspond to small spherical aggregates (0.06 Pa·s) rather it should have a structure of big globular micellar aggregates that become gel network in the cubic phase.

The introduction of the ***IrPa*** complex induces a small increase of the systems viscosity with temperature, more pronounced in the case of ***IrPa_Sol2*** mixture, indicating the participation of the chromophore guest to the micellar process formation (bigger micelles).

Furthermore, the effect of temperature has a strong impact in the dynamics of the system. The dynamic mechanical analysis (DMA) ability to give complex viscosity and G' and G" values for each point in a temperature scan, allows one to estimate the transition temperature and the mechanical behaviour. This has the advantage of telling how much fluid the material is at a given temperature, so one can determine mechanical moduli values change with temperature and transitions in materials. This includes not only the phase transitions, but also other transitions that occur in the polymer matrix.

In the cubic phase, the shear viscosity is a function of the applied shear rates.[5d] The decrease of the viscosity with the increase of the shear rate is observed and it results in a shear-induced orientation and deformation of the lyotropic domains, with deformed and elongated micelles aligned parallel to direction of the shear field.[5d]

In Figure 2, the temperature dependence of the complex dynamic viscosities for ***IrPa_Sol*** and ***Sol*** systems are shown. Both systems present similar cure profiles but the system containing ***IrPa*** shows slightly lower G* values for system 1. It is worthy to note that in both cases, the cubic phase presents other "transitions" at high temperatures. In fact, it is clear that the moduli do not follow a typical trend in temperature (slight decreasing for kinetics effects), a little jump indicating different structural organizations of the cubic phase (between 45 and 55°C). Although the phase diagram of F127 in water was intensely investigated, this peculiar behaviour was not reported until now.[4,8,9]

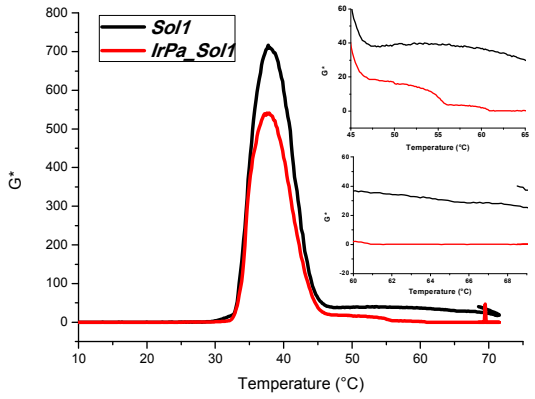

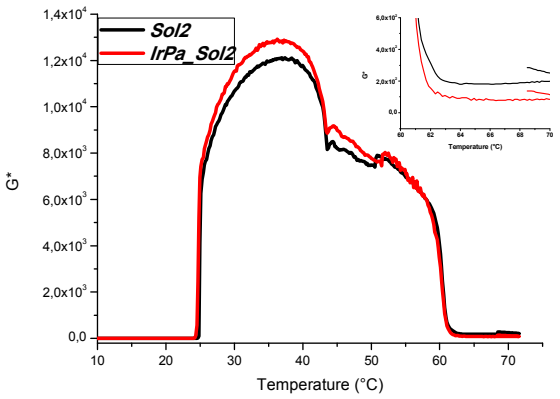

Figure 2. Linear viscoelastic thermograms for the investigated systems.

Furthermore, the 'melting' of the cubic lattice to the hexagonal symmetry phase at high temperature (60-70°C) is strongly marked by the falling of the both moduli.

The viscosity of ***IrPa*** complex in water was measured at the same concentration used to prepare our systems, and it shows values similar to water (10^{-3}Pa·s at 25°C). Obviously, the addition of ***IrPa*** on F127 mixtures has marked differences: the ***IrPa_Sol*** systems acquire the more gel-like properties of the polymeric system, and moreover, the polymeric networks of ***IrPa_Sol1*** and ***IrPa_Sol2*** become more solid than the blank solutions (***Sol1*** and ***Sol2***) in the micellar phase. This effect can be related to the increase of density of active links present in the polymer network.[4,6,11a]

The addition of ***IrPa*** does not affect strongly the polymer association process. Indeed, the cubic phase maintains his 'phase existence range', with a small decrease of the solid character in case of system 1, therefore a decrease of the inter-micelle interactions. This suggest that the ***IrPa*** chromophore is located in the micellar corona, thus hindering the interactions between the strongly packed micelles.[11a] In the case of system 2, again the higher polymer content seems to dominate, the effect of the ***IrPa*** being negligible.

Furthermore, the decrease of the hexagonal phase viscosity in both systems ***IrPa_Sol1*** and ***IrPa_Sol2*** compared with their blank solutions, ***Sol1*** and ***Sol2***, is observed (insets Figure 2). This implies a decreasing intermicelle interaction, probably because of the expulsion of the chromophore into water media from the less hydrophilic PEO corona, due to a dehydration process of the corona with increasing temperature.[8,9]

Self-diffusion. In order to obtain information on the influence of the ***IrPa*** complex on the aggregate nanostructures of F127, we performed accurate PGSE-NMR experiments, where the polymer self-diffusion (Ds) was measured as function of temperature during the termogelation process of the micellar aggregates (isotropic solution-to-micellar cubic phase).

To get information on the effects of the introduction of the ***IrPa*** complex in the F127-water system, we compared the variation of diffusion coefficients on ***Sol2*** and ***IrPa_Sol2*** respectively, with DSC and rheological experiments. The DSC signal of the two mixtures consists of a broad endothermic peak and is characterized by two temperatures: T_{onset}, which is the temperatures at which micellization of F127 starts and T_{max}, the temperature at the maximum of peak. As reported in Table 1, for the blank solution and the mixtures loaded with the Ir cromophore, both temperatures have small variation (system 1) or coincide (system 2). Rheological tests in temperature showed also identical behaviours which are characterized by the gel temperature isotropic/cubic (T_{gel} = 32°C for system 1 and respectively 24°C for system 2). Over this temperature, no Newtonian behaviour is observed and the cubic phase is formed (Figure 2).

In Figure 3, we report the temperature variation of polymer self-diffusion coefficients for the two aqueous mixtures, ***Sol2*** and ***IrPa_Sol2*** respectively. According to DSC and rheology, the self-diffusion measurements allow a very simple analysis.

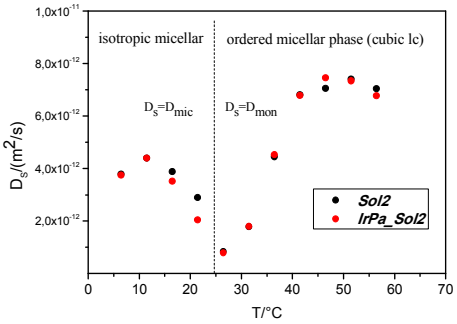

Figure 3. Polymer self-diffusion (Ds) vs temperature as measured by means of NMR Diffusometry for the two micellar solutions ***Sol2*** and ***IrPa_Sol2***. The dashed line corresponds to isotropic/ordered cubic structure as relived by visual observations of gelation point on thermal baths.

On increasing the temperature, the polymer diffusion coefficients show a sensitive decrease. For the temperature interval 5-25°C the measured D_s correspond to the diffusion of the spherical micelles (D_{mic}) whose size increases with increasing temperature. The diffusion coefficient measured at 26°C show a very low value (cca. $7.5x10^{-13}$ $m^2 \cdot sec^{-1}$) which accounts for the onset of gelification of solution. As a consequence of identical results on this temperature interval for the two mixtures, we can say that the complex does not present any effects on the growth and gelation of F127 micelles.

On the contrary, at temperatures above 26°C D_s show a remarkable change, consisting on a strong increase of mobility for both mixtures with increasing temperature. Therefore, if a picture of a cubic liquid crystalline phase (i.e. packed micelles of F127) is valid, one has to invoke another diffusion mechanism of the polymer, in order to accounts the increase of the diffusion against the gelification of the solution (as seen on rheothermograms). The only conceivable such mechanism is the exchange of polymer, either between aggregates and monomers or between discrete and immobile aggregates (D_{mon}). Both these processes may influence the measured self-diffusion coefficients.

Finally, at higher temperatures (ca. 45°C), the self-diffusion reaches a sort of plateau and the patterns for the two mixtures suggests the presence of strongly packed structures (at least also a multiconnected network of micelles) which is not affected by the presence of complex in solution.

Photophysical Measurements. In order to gain insights into the ***IrPa***–F127 system behaviour, a full photophysical investigation including emission spectra, phosphorescence quantum yield and time-resolved luminescence was conducted on both ***IrPa_Sol1*** and ***IrPa_Sol2*** mixtures (vide infra).

In particular, the photophysical properties were investigated for the mixtures at 22°C, where the surfactant is in the micellar phase and at 35°C where the cubic mesophase is completely formed. Finally, the photophysical properties of ***IrPa_Sol2*** mixture were further tested by increasing the temperature up to 75°C where the observed liquid crystalline phase was wholly destabilized. The full photophysical results are summarized in Tables 3 and 4.

Table 3. Luminescence properties of *IrPa _Sol1* mixture

	[a]λ_{em}/nm	[a]τ/ nsec	[a] ϕ
[a]**IrPa**	509 [b](484)	433	0.20
***IrPa _Sol1* 22°C**	493 [b](514)	τ_1 = 433 (14%) τ_2 = 760 (86 %)	0.34
***IrPa_Sol1* 35°C**	493 [b](514)	τ_1 = 404 (19 %) τ_2 = 660 (81 %)	0.28

[a]air equilibrated water solution; [b]emission band shoulder

Table 4. Luminescence properties of *IrPa_Sol2* mixture

	[a]λ_{em}/nm	[a]τ/ nsec	[a] ϕ
***IrPa _Sol2* 22°C**	493 [b](514)	τ_1 = 516 (12%) τ_2 = 960 (88 %)	0.44
***IrPa _Sol2* 35°C**	493 [b](514)	τ_1 = 457 (33 %) τ_2 = 694 (67 %)	0.31
***IrPa _Sol2* 45°C**	493 [b](514)	τ_1 = 365 (45 %) τ_2 = 523 (55 %)	0.21
***IrPa _Sol2* 65°C**	493 [b](514)	300	0.14
***IrPa _Sol2* 75°C**	493 [b](514)	216	0.10

[a]air equilibrated water solution; [b]emission band shoulder

Behaviour in the micellar phase. In air equilibrated water solution, ***IrPa*** complex showed a brilliant blue–green emission, with the emission maximum centred at 509 nm, a luminescence quantum yield (φ) of 0.20 and an emission lifetime of about 430 ns (Table 3) in agreement with previous data.[10a]

As reported in Tables 2 and 3, at 22°C, *i.e.* in the micellar phase, ***IrPa*** complex showed, with respect to water solution, a slight blue shift of the emission maximum and a significant increase of the luminescence quantum yield values for both ***IrPa _Sol1*** and ***IrPa _Sol2*** mixtures. Moreover in both cases, the luminescence decay showed a bi-exponential kinetic indicating an inhomogeneous distribution of the chromophore into the micellar phase.

In particular, ***IrPa_Sol1*** mixture showed a longer lifetime component of 760 ns accounting for the most of the signal (86%) and a shorter one of 433 ns that accounts for 14%. Analogously, ***IrPa_Sol2*** showed a longer component of 960 ns and a shorter one of 516 ns accounting for 88 % and 12% of the total decay respectively.

The slightly blue shift of the emission spectrum observed for **Ir** in both ***IrPa_Sol1*** and ***IrPa_Sol2*** mixture suggest that a different microenvironment is experienced by the chromophore when it is mixed with F127 based micelles with respect to water solution.[10] Moreover, since the longer luminescent lifetime component detected for ***IrPa*** at 22°C in both micellar phases is considerably longer with respect to the one observed in water solution, it can be associated to the presence into the two solutions of a large fraction of iridium(III) chromophores with a reduced nonradiative decay due to vibrational modes and/or partially shielded from oxygen that is known to efficiently quench iridium(III) complexes phosphorescence via energy transfer mechanism.[17]

While the shorter lifetime component suggests that a minor fraction of ***IrPa*** chromophores is still present into the water phase of the micellar solutions, the appearance of the longer one corroborate the presence of a large fraction of iridium chromophores strongly associated with the micellar structures. In particular, due to its polar/ionic nature, the iridium(III) complex selected for the present work, when dissolved in pluronic F127 based micelles, should be preferentially located into the polar corona region of the micelles. This location should result, with respect to water solution, mainly in an enhancement of the local friction experienced by the iridium(III) chromophores, hypothesis in agreement with the observed photophysical results.

Finally, the increase of lifetime values observed for ***IrPa_Sol2*** with respect to ***IrPa_Sol1*** at 22°C can be attributed to the increase of the overall viscosity detected for ***IrPa_Sol2*** which more effectively contribute to reduce molecular vibration.

Behaviour in the cubic phase. On moving from the micellar phase (22°C) to the cubic mesophase (35°C), no change in the emission energy for ***IrPa*** complex luminescence was observed for both ***IrPa_Sol1*** and ***IrPa_Sol2*** mixtures (Tables 3-4). Moreover the luminescence quantum yield values resulted to be significantly lower. Regarding the luminescence lifetime, at 35°C, all the recorded decays still retain a bi-exponential kinetic for both the mixtures, while the lifetime constants resulted all significantly shorter. F127 gelation is associated to a polymer dehydration process resulting in an increase of chain

friction and entanglement and producing hydrophobic association.[8,9] As a consequence, the corona region undergoes to a drastic enhancement of the local friction during such a process. Taking into account the preferential affinity of ***IrPa*** for the polar corona region, as a consequence of gelation, an increase of the luminescence quantum yield and lifetime values associated to an enhancement of the iridium(III) chromophores rigidity is expected.

Nevertheless at 35°C, where the cubic mesophase is completely formed, both ***IrPa_Sol1*** and ***IrPa_Sol2*** mixtures showed a significant decrease of both luminescence lifetimes and quantum yields. In particular while a slight decrease of the lifetime value associated to the minor fraction of iridium(III) chromophores located into the water phase can be ascribed to the increase of temperature and therefore to thermal agitation, the more drastic decrease of the lifetime values showed by the chromophores associated to the micellar structures strongly suggest the activation of a further quenching mechanism strongly related to the mesophase formation. Indeed, as a consequence of gelation, the micellar entanglement should favour the establishment of shorter inter-chromophoric distance between the iridium(III) chromophores located into the corona region promoting the activation iridium(III) luminescence self-quenching phenomena.[11a, 18]

As expected, by increasing the temperature of ***IrPa_Sol2*** mixture up to 75°C, both luminescence quantum yield and lifetimes values showed a progressive decrease mainly do to an enhancement of the molecular mobility and of the all the non-radiative processes related to thermal agitation. Moreover, an interesting behaviour is observed. As pointed out by the data reported in Table 2, with increasing temperature, a progressive alignment of the relative amplitude values associated to the bi-exponential luminescence decays toward a single value is also detected. The present behaviour seems to indicate the progressive modification of the supramolecular organization of the mixture toward a situation where each ***IrPa*** chromophore experiences the same molecular environment. Reasonably, the progressive polymeric dehydration process associated to the increase of temperature, strongly modify the polarity of the corona microenvironment. Consequently, due to its polar/ionic nature, the selected ***IrPa*** complex cannot longer be hosted into such a region and it is progressively push out into the water phase where it is finally subjected only to the effect of temperature.

Conclusions

This study aimed the detection of the position of a hydrophilic ionic iridium(III) chromophore (***IrPa***) inside the micellar, cubic and hexagonal dynamic system of the F127 phase diagram in water, effectively accomplished by the convenient combination of different techniques, such as DSC, rheology, self-diffusion measurements and photophysics.

We successfully built highly ordered luminescent systems in which the iridium(III) chromophore is well-dispersed into the corona region of the micelles forming the micellar and cubic phases. The iridium(III) chromophores remained stable into the corona region until the formation of the hexagonal phase (60-70°C) when, due to the increased hydrophobicity of the micelle, they are expelled into the water media.

With respect to the previously studied ***Ir12***-F127 systems, the good solubility of ***IrPa*** in water solution, allowed us to avoid the use of a co-solvent for the complex solubilisation. Furthermore the different solubility showed by the two iridium(III) complexes allowed us to functionalize preferentially the F127 micellar core in the case of ***Ir12*** (Figure 1a) previously reported,[11a] and the F127 micellar corona in the in the case of ***IrPa*** (Figure 1b).

In conclusion, the systems presented can be effectively used as functional templates for the construction of mesostructured materials with well-dispersed iridium(III) emitters, in which the position of the cromophore is predetermined, yielding materials with functional pores or walls, as a function of the position of the chromophore in the initial lyotropic templated system.

Acknowledgements

This work was supported by the European Community's Seventh Framework Program (FP7 2007–2013), through MATERIA project (PONa3_00370). Dr E. I. Szerb further acknowledges the European Union and Regione Calabria (Fondo Sociale Europeo, POR Calabria FSE 2007/2013) for partial funding.

Notes and references

[a] LASCAMM CR-INSTM Unità della Calabria, Dipartimento di Chimica e Tecnologie Chimiche - CTC, Università della Calabria, Via P. Bucci Cubo 14C, Arcavacata (CS) 87036, Italy. **e-mail address: cesare.oliviero@unical.it*
[b] University 'Politehnica' of Bucharest, Faculty of Applied Chemistry and Materials Science, "Costin Nenitescu" Department of Organic Chemistry, 1-7 Polizu St., Bucharest, Romania.
[c] CNR IPCF UOS Cosenza Università della Calabria, Via P. Bucci Cubo 14C , Arcavacata (CS) , 87036 , Italy.

1 (a) M. Malmsten, *Soft Matter*., 2006, **2**, 760-769; (b) G. Tiwari, R. Tiwari, B. Sriwastawa, L. Bhati, S. Pandey, P. Pandey and S. K. Bannerjee, *Int. J. Pharm. Investig*., 2012, **2**, 2-11; (c) E. A. Yapar and Ö. İnal, *Trop J Pharm Res,* 2012*,* **11***,* 855-866; (d) S. dos Santos, B. Medronho, T. dos Santos and F. E. Antunes, *Drug Delivery Systems: Advanced Technologies Potentially Applicable in Personalised Treatment, Advances in Predictive, Preventive and Personalised Medicine 4*, J. Coelho (ed.), © Springer ScienceCBusiness Media Dordrecht, 2013.

2 (a) N. Garti, A. Spernath, A. Aserin and R. Lutz, *Soft Matter*., 2005, **1**, 206-218; (b) J. Weiss, P. Takhistov and J. McClements, *J. of Food Sci*., 2006, **71**, R107-R116; (c) I. Lacatusu, N. Badea, R. Stan and A. Meghea, *Nanotechnology*, 2012, **23**, 455702(13pp).

3 (a) F. Hoffmann, M. Cornelius, J. Morell and M. Fröbam, *Angew. Chem. Int. Ed*., 2006, **45**, 3216-3251; (b) Y. Wan and D. Zhao, *Chem. Rev*., 2007, **107**, 2821-2860; (c) C. Wang, D. Chen and X. Jiao, *Sci. Technol.* Adv. Mater., 2009, **10**, 023001(11pp); (d) J. L. Vivero-Escoto, Y.-D. Chiang, K. C.-W. Wu and Y. Yamauchi, Sci. Technol.

Adv. Mater., 2012, **13**, 013003(9pp); (e) R. Zhang, A. A. Elzatahry, S. S. Al-Deyab an D. Zhao, *Nano Today*, 2012, **7**, 344-366.

4 P. Alexandridis and T. A. Hatton, Colloids Surfaces A: Physicochem. Eng. Aspects, 1995, **96**, 1-46;

5 (a) R. L. Rill, Y. Liu, D. H. Van Winkle and B. R. Locke, *J. Chromatography A*, 1998, **817**, 287-295; (b) R. Nagarajan, *Colloids Surf. B,* 1999, **16**, 55-72; (c) J. Escobar-Chávez, M. López-Cervantes, A. Naïk, Y. N. Kalia, D. Quintanar-Guerrero and A. Ganem-Quintanar, *J. Pharm. Pharmaceut. Sci*., 2006, **9**, 339-358; (d) F. E. Antunes, L. Gentile, C. O. Rossi, L. Tavano and G. A. Ranieri, *Colloids Surf. B*, 2011, **87**, 42-48.

6 (a) P. Alexandridis and J. F. Holzwarth, *Langmuir*, 1997, **13**, 6074-6082; (b) P. Holmqvist, P. Alexandridis and B. Lindman, *Macromolecules*, 1997, **30**, 6788-6797; (c) P. Holmqvist, P. Alexandridis and B. Lindman, Langmuir, 1997, **13**, 2471-2479; (d) R. Ivanova, B. Lindman and P. Alexandridis, *Langmuir*, 2000, **16**, 3660-3675; (e) P. Alexandridis, R. Ivanova and B. Lindman, *Langmuir*, 2000, **16**, 3676-3689; (f) R. Ivanova, B. Lindman and P. Alexandridis, *Langmuir*, 2000, **16**, 9058-9069; (g) R. Ivanova, P. Alexandridis and B. Lindman, *Colloids and Surfaces A: Physicochem. Eng. Aspects*, 2001, **183–185**, 41-53; (h) P. Parekh, J. Dey, S. Kumar, S. Nath, R. Ganguly, V. K. Aswal and P. Bahadur, *Colloids Surf., B*., 2014, **114**, 386 – 391.

7 L. Mahoney and R. T. Koodali, *Materials,* 2014, **7**, 2697-2746.

8 (a) M. Malmsten and B. Lindman, *Macromolecules*, 1992, **25**, 5446-5450; (b) P. Holmqvist, P. Alexandridis and B. Lindman, *J. Phys. Chem. B*, 1998, **102**, 1149-1158; (c) H. Walderhaug, *J. Phys. Chem. B,* 1999, **103**, 3352-3357; (d) Y. Ding, Y. Wang and R. Guo, *J. Disper. Sci. Technol*., 2003, **24**, 673-681;

9 (a) G. Wanka, H. Hoffmann and W. Ulbricht, *Colloid Polym. Sci*., 1990, **268**, 101-117; (b) G.-E. Yu, Y. Deng, S. Dalton, Q.-G. Wang, D. Attwood, C. Price and C. Booth, *J. Chem. Soc. Faraday Trans*., 1992, *88*, 2537 – 2544; (c) G. Wanka, H. Hoffmann and W. Ulbricht, *Macromolecules*, 1994, **27**, 4145; (d) L. Gentile, G. De Luca, F. Antunes, C. Oliviero Rossi, G. A. Ranieri, *Appl. Rheol*., 2010, **20**, 52081-52089.

10 (a) Y. J. Yadav, B. Heinrich, G. De Luca, A. M. Talarico, T. F. Mastropietro, M. Ghedini, B. Donnio and E. I. Szerb, *Adv. Optical Mater.,* 2013, **1**, 844–854 and references therein; (b) A. M. Prokhorov, A. Santoro, J. A. G. Williams and D. W. Bruce , *Angew. Chem. Int. Ed.,* 2012, ***51***, 95-98; (c) C. H. Shin, J. O. Huh, M. H. Lee and Y. Do, *Dalton Trans.,* 2009, 6476-6479; (d) H. Wang, Q. Liao, H. Fu, Y. Zeng, Z. Jiang, J. Ma and J. Yao, *J. Mater. Chem.,* 2009, ***19***, 89-96; (e) H. J. Bolink, L. Cappelli, S. Cheylan, E. Coronado, R. D. Costa, N. Lardies, Md. K. Nazeeruddin and E. Orti, *J. Mater. Chem.,* 2007, **17**, 5032-5041.

11 (a) A. M. Talarico, M. Ghedini, C. Oliverio Rossi and E. I. Szerb, *Soft Matter*, 2012, **8**, 11661-11669; (b) D. Aiello, A. M. Talarico, F. Teocoli, E. I. Szerb, I. Aiello, F. Testa and M. Ghedini, *New J. Chem*., 2011, **35**, 141-148; (c) M. Mauro, G. De Paoli, M. Otter, D. Donghi , G. D'Alfonso and L. De Cola, *Dalton Trans.,* 2011, **40**, 12106-12116; (d) A. Guerrero-Martınez, Y. Vida, D. Domınguez-Gutierrez, R. Q. Albuquerque and L. De Cola, *Inorg. Chem.,* 2008, **47**, 9131-9133.

12 T. F. Mastropietro, Y. J. Yadav, E. I. Szerb, A. M. Talarico, M. Ghedini and A. Crispini, *Dalton Trans*., 2012, **41**, 8899-8907.

13 E. O. Stejskal, J. E. Tanner, *J. Chem. Phys*., 1965, **42**, 288-292.

14 (a) J. K. M. Sanders, B. K. Hunter, *Modern NMR Spectroscopy*, Oxford University Press, Oxford, 1987, 61–67; (b) C. Oliviero, L. Coppola, C. La Mesa, G.A. Ranieri and M. Terenzi, *Colloids and Surfaces A*, 2002, **201**, 247-260.

15 (a) J. A. Bevis, R. Bottom, J. Duncan, I. A. Farhat, M. J. Forrest, D. Furniss, P. Gabbott, B. MacNaughtan, S. N. Nazhat, M. Saunders and A. Seddon, *Principles and Applications of Thermal Analysis,* ed P. Gabbott, Blackwell Publishing Ltd, ISBN-13: 978-1-4051-3171-1, 2008; (b) L. Gentile, L. Filippelli, C. Oliviero Rossi, N. Baldino and G. A. Ranieri, *Mol. Cryst. Liq. Cryst*., 2012, **558**, 1–10.

16 (a) N. Demas and G. A. Crosby, *J. Phys. Chem*., 1971, **75**, 991-1024; (b) K. Nakamaru, *Bull. Chem. Soc. Jpn*., 1982, **55**, 2697-2705.

17 D. Ashen-Garry and M. Selke, *Photochemistry and Photobiology*, 2014, **90**, 257–274 and reference therein.

18 Y. Kawamura, J. Brooks, J. J. Brown, H. Sasabe and C. Adachi, *Phys. Rev. Lett*., 2006, **96**, 017404-4.

